THE JOURNAL OF BIOLOGICAL CHEMISTRY VOL. 289, NO. 15, pp. 10293–10307, April 11, 2014

A Mouse Model for Dominant Collagen VI Disorders

*HETEROZYGOUS DELETION OF Col6a3 EXON 16**

Received for publication, January 9, 2014, and in revised form, February 10, 2014 Published, JBC Papers in Press, February 22, 2014, DOI 10.1074/jbc.M114.549311

Te-Cheng Pan[‡], Rui-Zhu Zhang[‡], Machiko Arita[‡], Sasha Bogdanovich[§], Sheila M. Adams[¶], Sudheer Kumar Gara[‖], Raimund Wagener[‖], Tejvior S. Khurana[§], David E. Birk[¶], and Mon-Li Chu[‡1]**

*From the [‡]Department of Dermatology and Cutaneous Biology, Thomas Jefferson University, Philadelphia, Pennsylvania 19107, [§]Department of Physiology and Pennsylvania Muscle Institute, University of Pennsylvania School of Medicine, Philadelphia, Pennsylvania 19104, [¶]Department of Molecular Pharmacology and Physiology, University of South Florida, Morsani College of Medicine, Tampa, Florida 33612, and [‖]Center for Biochemistry and **Center for Molecular Medicine, Medical Faculty Cologne, University of Cologne, Cologne D-50931, Germany*

Background: Dominant collagen VI gene mutations cause the severe Ullrich congenital muscular dystrophy (UCMD) and mild Bethlem myopathy.
Results: A mutant mouse mimicking the most common molecular defect in dominant UCMD patients was generated and characterized.
Conclusion: The mutant mouse displays muscle and connective tissue abnormalities.
Significance: The mutant mouse provides an animal model for dominant collagen VI disorders.

Dominant and recessive mutations in collagen VI genes, *COL6A1*, *COL6A2*, and *COL6A3*, cause a continuous spectrum of disorders characterized by muscle weakness and connective tissue abnormalities ranging from the severe Ullrich congenital muscular dystrophy to the mild Bethlem myopathy. Herein, we report the development of a mouse model for dominant collagen VI disorders by deleting exon 16 in the *Col6a3* gene. The resulting heterozygous mouse, *Col6a3*$^{+/d16}$, produced comparable amounts of normal *Col6a3* mRNA and a mutant transcript with an in-frame deletion of 54 bp of triple-helical coding sequences, thus mimicking the most common molecular defect found in dominant Ullrich congenital muscular dystrophy patients. Biosynthetic studies of mutant fibroblasts indicated that the mutant α3(VI) collagen protein was produced and exerted a dominant-negative effect on collagen VI microfibrillar assembly. The distribution of the α3(VI)-like chains of collagen VI was not altered in mutant mice during development. The *Col6a3*$^{+/d16}$ mice developed histopathologic signs of myopathy and showed ultrastructural alterations of mitochondria and sarcoplasmic reticulum in muscle and abnormal collagen fibrils in tendons. The *Col6a3*$^{+/d16}$ mice displayed compromised muscle contractile functions and thereby provide an essential preclinical platform for developing treatment strategies for dominant collagen VI disorders.

Collagen VI is a microfibrillar extracellular matrix (ECM)[2] protein found in almost all tissues. Triple-helical collagen VI monomers consist of three different α chains (1). Monomers made up of the α1(VI), α2(VI), and α3(VI) chains are the most abundant and best characterized. Each α chain is composed of a central triple-helical domain of 335 or 336 amino acids with a repeating Gly-*X*-*Y* amino acid sequence (2), which is flanked by N- and C-terminal globular domains mainly composed of von Willebrand factor type A modules (3, 4) (Fig. 1*A*). The N- and C-globular domains of the α3(VI) chain are much larger than those in the α1(VI) and α2(VI) chains. As a consequence, the α3(VI) chain is about 3 times the size of the α1(VI) and α2(VI) chains (~3000 *versus* ~1000 amino acids). The triple-helical collagen VI monomers undergo intracellular assembly into dimers and tetramers and are then secreted (Fig. 1*B*). In the extracellular space, tetramers associated end-to-end into collagen VI microfibrils, which display a characteristic double-beaded structure (1). A strategic single cysteine residue in the triple-helical domain and short cysteine-rich segments flanking the triple-helical domain of each chain are essential for the assembly and stability of collagen VI dimers, tetramers, and microfibrils (2–4) (Fig. 1, *A* and *B*). Three α3(VI)-like α chains, α4(VI), α5(VI), and α6(VI), have been identified in different animal species in recent years (5, 6) (Fig. 1*A*). Humans do not produce the α4(VI) protein because the gene is inactivated by a chromosomal translocation. These α3(VI)-like chains can substitute the α3(VI) chain in the assembly of collagen VI, but they have rather restricted tissue distributions (7).

Dominant and recessive mutations in the *COL6A1*, *COL6A2*, and *COL6A3* genes lead to a continuous spectrum of disorders characterized by muscle weakness and connective tissue abnormalities. Ullrich congenital muscular dystrophy (UCMD, OMIM #254090), the severe end of the clinical spectrum caused by an absence or marked deficiency of collagen VI, is currently recognized as one of the most common types of congenital muscular dystrophies (8–11). Apart from muscle weakness,

* This work was supported, in whole or in part, by National Institutes of Health Grants AR053251 (to M.-L. C.) and AR44745 (to D. E. B.). This work was also supported by the German Research Foundation (SFB829; to R. W.).
[1] To whom correspondence should be addressed: Dept. of Dermatology and Cutaneous Biology, Thomas Jefferson University, 233 South 10th St., Philadelphia, PA 19107. Tel.: 215-503-4834; Fax: 215-503-5788; E-mail: mon-li.chu@jefferson.edu.
[2] The abbreviations used are: ECM, extracellular matrix; UCMD, Ullrich congenital muscular dystrophy; FDL, flexor digitorum longus; EDL, extensor digitorum longus; ECC, eccentric contractions; TH, triple-helical domain; Bis-Tris, 2-[bis(2-hydroxyethyl)amino]-2-(hydroxymethyl)propane-1,3-diol.

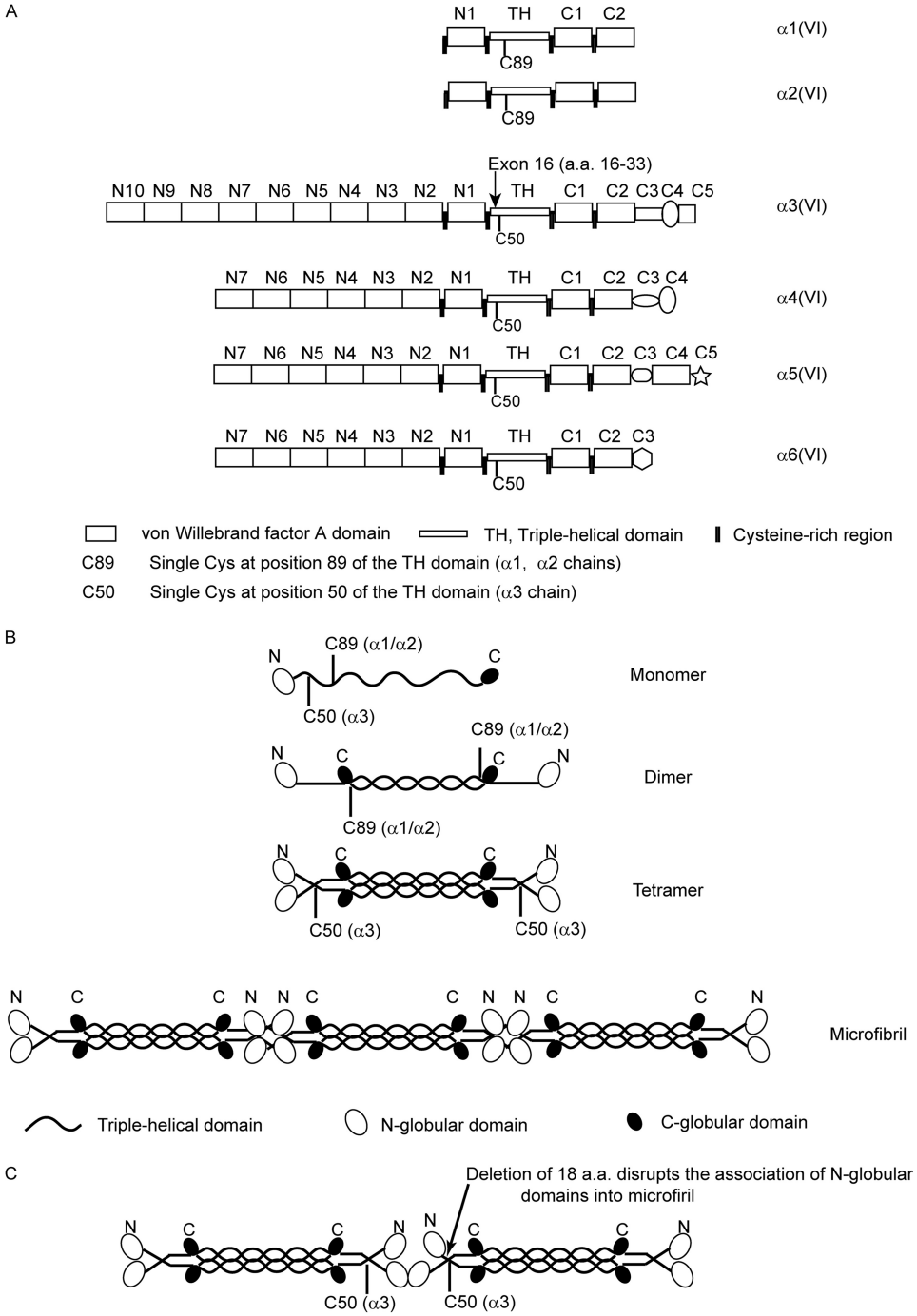

FIGURE 1. **Schematic diagram of collagen VI chains, microfibrillar assembly, and consequence of in-frame triple-helical deletions.** *A*, modular structures of collagen VI chains. Each chain contains a similar sized triple-helical domain (TH) of 335–336 amino acids flanked by N- and C-globular domains consisting mainly of von Willebrand factor type A domains (N1-N10, C1-C2). A single cysteine residue present in the TH domain of each chain is located at position 89 (*C89*) in the triple-helical domain of the α1 and α2 chains and at position 50 (*C50*) of the α3, α4, α5, and α6 chains. Deletion of *Col6a3* exon 16 removes amino acids 16–33 of the TH domain. *B*, assembly of collagen VI microfibrils. The α1, α2, and α3 chains assemble into a dumbbell-shaped collagen VI monomer with a central triple helix flanked by N- and C-globular domains. Two monomers associate in a staggered anti-parallel fashion into a dimer with the N-globular domains protruding. Two dimers associate in parallel into a tetramer, which is then secreted. In the extracellular space tetramers associate end-to-end via the N-globular domains into a microfibril. *C*, consequence of in-frame deletion in the N terminus of the triple-helical domain. As triple helix folding proceeds from the C to N terminus, mutant monomers, dimers, and tetramers are formed. However, microfibrils cannot be assembled when the N-terminal region of the tetramer is abnormal. *a.a.*, amino acids.

UCMD patients display connective tissue defects, including joint contractures, distal hyperlaxity, and skeletal anomalies (scoliosis, kyphosis, torticollis, spinal stiffness, and Achilles tendon contractures) (8, 9). In addition, skin abnormalities, *e.g.* velvety skin, hyperkeratosis, and keloid formation, are common. Severely affected patients either never achieve independent ambulation or can walk initially, but the ability is lost by the teen years (8, 12, 13). Respiratory insufficiency develops progressively, and ultimately patients almost invariably need ventilation support. Bethlem myopathy (OMIM #158810),

resulting from dominant collagen VI mutations primarily, is at the mild end of the clinical spectrum (8, 9). Due to a slowly progressive clinical course, more than two-thirds of the Bethlem myopathy patients over 50 years of age require aids for ambulation (14). Mutations in collagen VI also underlie disease phenotypes intermediate between classical UCMD and Bethlem myopathy, limb-girdle muscular dystrophy, and myosclerosis (OMIM #255600) (8, 9, 15, 16). Mutations in the *COL6A5* and *COL6A6* genes have not been described to date.

Severe UCMD phenotypes are caused by either recessive or dominant negative collagen VI gene mutations (17, 18). The recessive UCMD patients typically bear homozygous or compound heterozygous nonsense or frameshift mutations, which trigger nonsense-mediated mRNA decay and thus result in complete absence or drastic reduction of collagen VI (8, 9, 19). Haploinsufficiency in collagen VI usually does not lead to a disease phenotype as almost all family members of the recessive UCMD patients who carry heterozygous mutations are healthy (17). However, variable penetrance of a nonsense mutation in a family has been reported, suggesting the presence of genetic modifiers (20). A mouse mutant lacking the α1(VI) chain of collagen VI, the *Col6a1* null mouse, has served as an animal model for recessive UCMD (21). Recently, we described a *Col6a3* mutant mouse, *Col6a3*$^{hm/hm}$, which lacks normal α3(VI) chain but produces a low level of non-functional α3(VI) chain (22). The *Col6a1* null and *Col6a3*$^{hm/hm}$ mice both display relatively mild myopathic pathology and have normal life spans. Thus, the mouse models for recessive collagen VI disorders have substantially milder phenotypes than the patients.

De novo dominant collagen VI gene mutations have been found in more than half of the severely affected UCMD patients studied to date (8, 9). These patients often carry a heterozygous mutation in one of the three collagen VI genes that affects the amino acid sequence in the N-terminal region of the triple-helical domain before the single cysteine (18, 23–25). The mutations are either splice site mutations that cause small in-frame deletions in the triple-helical domains or missense changes that alter the obligatory glycine residues of the repetitive Gly-*X*-*Y* sequences. In contrast to the total absence or severe deficiency of collagen VI in recessive UCMD, abnormal collagen VI protein is abundantly present in the interstitial connective tissue between muscle fibers in the dominant UCMD patients (18). The pathological mechanisms and treatment strategies for the dominant and recessive patients are not identical. For instance, the presence of mutant collagen VI in the endomysium likely alters the muscle extracellular microenvironment, which in turn may influence the cellular activities of the adjacent muscle cells in a manner that differs from the total absence of collagen VI protein in recessive UCMD. Moreover, silencing the mutant allele can be explored as a treatment strategy for dominant UCMD and Bethlem myopathy patients. To our knowledge an animal model for dominant collagen VI disorders has not been described. In this study we generated a mutant mouse bearing the most common molecular defect found in dominant UCMD patients, *i.e.* skipping of exon 16 in the *COL6A3* mRNA (11, 13, 23, 25). We show that mutant mice heterozygous for the *Col6a3* exon 16 deletion, named *Col6a3*$^{+/d16}$, display muscle and connective tissue abnormalities resembling, albeit milder than, the dominant UCMD patients.

EXPERIMENTAL PROCEDURES

Col6a3 Gene Targeting—A mouse 129/Sv genomic cosmid clone encoding part of the *Col6a3* gene was used to prepare the gene targeting construct (Fig. 2*A*). Exon 16 coding region was replaced by a neomycin resistance gene driven by the phosphoglycerol kinase promoter (PGK-Neo) and flanked by *loxP* sequences. The targeting vector contained a 6.1-kb DraIII fragment as the long arm, a 2.5-kb HindIII fragment as the short arm, and a diphtheria toxin A gene for negative selection. The targeting construct was linearized with SacII and electroporated into mouse 129/Sv embryonic stem cells. Neomycin-resistant cell clones were screened by Southern blotting using BglI-cut genomic DNA and a 0.7-kb external probe generated by PCR from the genomic subclone with primers GAGAGGAGATGTCGGGATTCG and GTGAGGCAGCAATGATGTAGAG. Two correctly targeted embryonic stem clones (wild type, 5.8 kb; mutant, 3.6 kb) were injected into mouse C57BL/6 blastocysts to generate chimeric mice, which were crossed with wild-type C57BL/6 mice to obtain germ-line transmission of a targeted allele, *Col6a3*^{d16N}, which contained the neomycin resistance gene (Fig. 2*A*). The heterozygous *Col6a3*$^{+/d16N}$ mice were crossed with transgenic mice bearing a Cre recombinase gene driven by a β-actin gene promoter to delete the neomycin resistance gene, yielding the final targeted allele, *Col6a3*^{d16}. Heterozygous mutant mice, *Col6a3*$^{+/d16}$, were backcrossed to C57BL/6 mice for 10 generations. Genotyping of the mice was performed by PCR. Forward primer CACTGCGGCAGATTAGGACT and reverse primer CCAGACAGGCTACAAACTCCA yielded an ~450-bp product from the *Col6a3*^{d16} allele and a faint 834-bp band from the wild type allele. Forward primer GCATACCTAGGCAGCCTCAC and the same reverse primer generated a 399-bp PCR product from the wild type allele but no product from the targeted allele.

Fibroblasts, RNA Isolation, RT-PCR, and DNA Sequencing—Primary fibroblast cultures were established from littermates of the three genotypes at embryonic day 17 following standard protocols and grown in DMEM with 10% fetal bovine serum (Invitrogen). Total RNA was prepared from confluent fibroblasts using the RNAeasy mini kit (Qiagen). RT-PCR of the mRNA encompassing the exon 16 coding region was carried out using forward primer TCTTGAACGTGTGGCTAACC and reverse primer CTTTTCTCCAGAAGAACCAGG. The resultant PCR products from homozygous and wild type cells were treated with ExoSAP-IT (Affymetrix) and subject to DNA sequencing using BigDye Terminator kit and 3730 DNA Sequencer (Applied Biosystems).

Collagen VI Biosynthesis—Embryonic fibroblasts were metabolically labeled with [^{35}S]cysteine in serum-free medium containing 50 μg/ml sodium ascorbate overnight as described (18). Culture medium and cell lysate were immunoprecipitated with an antibody specific for the α1(VI) chain (26) as described previously (18). The precipitated material was analyzed after reduction with 25 mM dithiothreitol on 3–8% polyacrylamide gels (NuPAGE Novex Tris-acetate gel, Invitrogen) or without

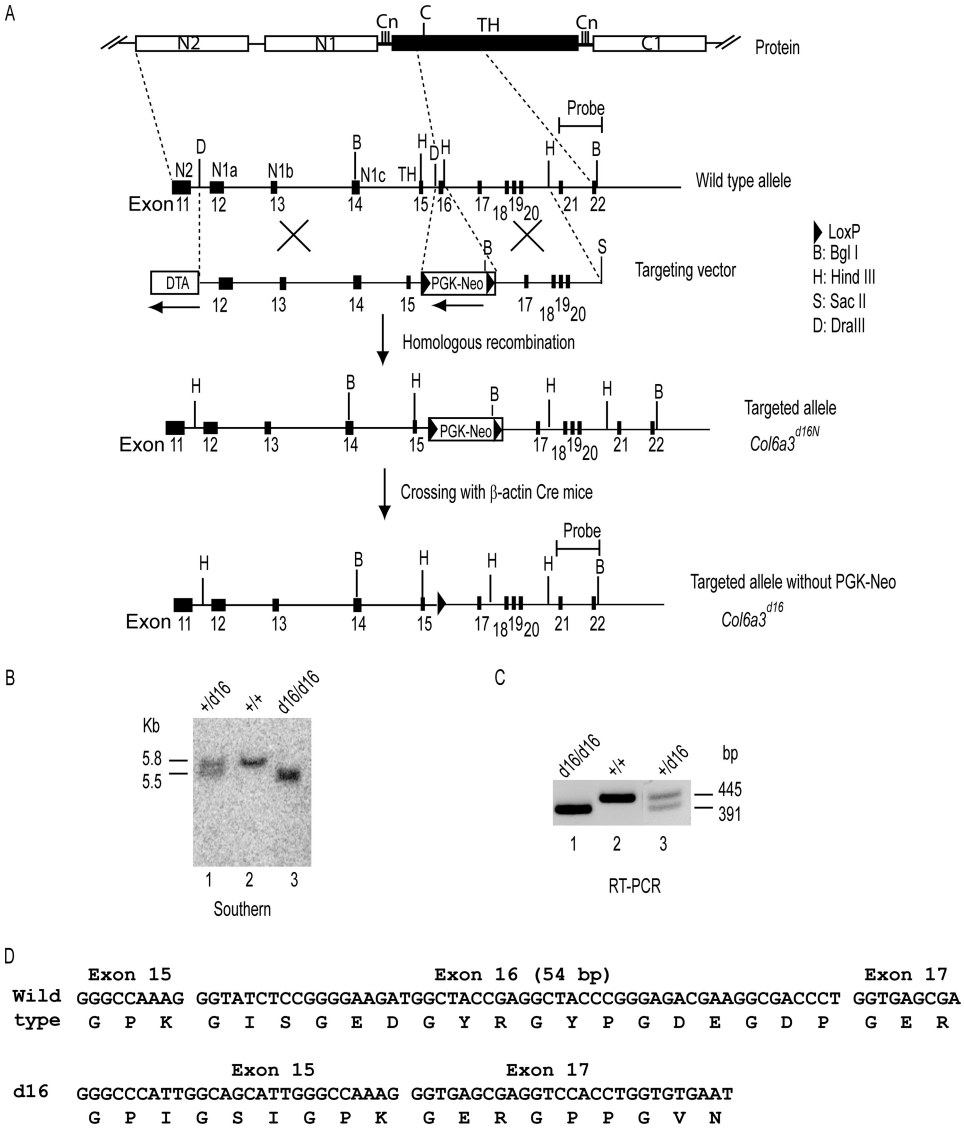

FIGURE 2. **Generation of mice bearing *Col6a3* exon 16 deletion.** *A*, targeting strategy. The gene-targeted region corresponds to exon 12–20 (exons as *black boxes*) of the wild type allele, which encodes the Willebrand factor type A module N1 in the N-terminal globular domain and part of the TH domain. *C*, single cysteine residue in the TH domain. *Cn*, cysteine-rich segments flanking the TH domain. The external probe used for Southern blotting and key restriction enzymes sites are shown. In the targeting vector exon 16 (54 bp) and its flanking intron sequences were replaced by the pGK-Neo gene flanked by *loxP* sequences (inserted in the opposite direction of *Col6a3* transcription), and a diphtheria toxin A (*DTA*) gene was included for negative selection. Homologous recombination generated the targeted allele (*Col6a3*^{d16N}), in which exon 16 was deleted and the pGK-Neo gene was present in the intron. Crossing of the *Col6a3*$^{+/d16N}$ mice with transgenic mice bearing a Cre recombinase gene driven by the β-actin promoter generated the *Col6a3*^{d16} allele, in which the PGK-Neo gene in the *Col6a3*^{d16N} allele was deleted and a *loxP* sequence (*black triangle*) remained in the targeted allele. *B*, Southern blot analysis of tail DNA from the *Col6a3*$^{+/+}$, *Col6a3*$^{+/d16}$, and *Col6a3*$^{d16/d16}$ mice. *C*, RT-PCR analysis of total RNA from the *Col6a3*$^{d16/d16}$, *Col6a3*$^{+/+}$, and *Col6a3*$^{+/d16}$ fibroblasts. *D*, DNA and amino acid sequences of the wild type and mutant *Col6a3* mRNA showing the in-frame deletion of the exon 16 coding region in the mutant allele. Note that a space is inserted in the exon borders.

reduction on composite 0.5% agarose and 2.4% polyacrylamide gels (18).

Western Blot Analysis—Tissues were frozen in liquid nitrogen and disrupted using a stainless steel pulverizer pre-chilled in liquid nitrogen. The resultant tissue powder was lysed in cold RIPA buffer (20 mM Tris-HCl (pH 7.5), 150 mM NaCl, 1% Nonidet P-40, 1% sodium deoxycholate, 1 mM EDTA, 1 mM EGTA, 2.5 mM sodium pyrophosphate, 1 mM β-glycerophosphate, 1 mM PMSF, 1 mM Na_3VO_4, 1 mM NaF, and 1 μg/ml each of aprotinin, leupeptin, and pepstatin), incubated at 4 °C for 4 h with slow rotation, sonicated for 15 s twice, and then centrifuged at 14,000 $\times$ *g* for 10 min. Protein concentration of the tissue lysate was determined using the Bio-Rad protein assay kit. Equal amounts of total proteins were run on 4–12% NuPAGE Novex Bis-Tris gels and blotted onto PVDF membranes. The blots were incubated with primary antibodies at 4 °C overnight and developed with the ECL plus reagent (GE Healthcare). Antibodies used were polyclonal antibodies against α1(VI) and α3(VI) chains (26, 27) and β-actin (Sigma).

Histology and Immunostaining—Mouse embryos and tails were frozen in OCT compound (VWR International). Dissected muscles from postnatal mice were mounted on 10% gum tragacanth (Sigma) and frozen in liquid nitrogen-cooled isopentane. Sections of 6–8-μm were stained with hematoxylin-eosin. Measurement of single muscle fiber area and percentage

of muscle fiber with central nuclei was performed as previously described (22). For immunostaining, cryosections were fixed with methanol and incubated with primary antibodies for 2 h at room temperature. The antibody reaction was detected with Cy3-labeled secondary antibodies (Jackson ImmunoResearch Laboratories). Fluorescence intensity of immunostained sections was measured using ImageJ software. Sections were also stained with DAPI to visualize nuclei. Immunostaining of fibroblasts was performed using cells grown in the presence of 50 μg/ml sodium ascorbate for 4 days post-confluency as described (18). Primary antibodies used were polyclonal antibodies against collagen VI α1, α3, α4, α5, and α6 chains (7, 26, 27), collagen I (Fitzgerald Industries International), tenascin-X (from Dr. Ken-Ichi Matsumoto), and periostin (R&D Systems). Samples were viewed using a Zeiss Axioskop epifluorescence microscope with a Toshiba 3CCD camera and ImagePro software (Media Cybernetics).

Physiological Analysis—Physiological studies were performed using female mice by methods described previously (28, 29). Briefly, weights of body, organs, and muscles were determined. Freshly dissected extensor digitorum longus (EDL) muscles were mounted between a force transducer and length controller in an organ bath containing oxygenated Ringer's solution (pH 7.4) at room temperature. Muscle length was adjusted to achieve maximal twitch and tetanic response, and optimal length was determined. Muscles were subject to a series of three twitches, three tetanic contractions, and five eccentric contractions (ECCs) at a total duration of 700 ms with the muscle being lengthened by 10% of optimal length at velocity of 0.5 optimal length(s) for mechanical property evaluation. ECC force decrement was calculated by the difference of isometric phase (500 ms) of the first and fifth ECCs. The cross-sectional area was determined using the Brooks-Faulkner approximation (30).

Electron Microscopy—Flexor digitorum longus (FDL) and Achilles tendons, and gastrocnemius muscles were dissected from 1-month-old mice and analyzed by transmission electron microscopy as previously described (31). Briefly, tissues were fixed in 0.1 M cacodylate buffer (pH 7.4) containing 4% paraformaldehyde, 2.5% glutaraldehyde, and 8 mM $CaCl_2$ and then post-fixed with 1% osmium tetroxide. Thin sections were post-stained with 2% aqueous uranyl acetate and 1% phosphotungstic acid (pH 3.2) and examined at 80 kV using a Tecnai 12 or JEOL 1400 transmission electron microscope equipped with a Gatan Ultrascan US100 2K digital camera or Gatan Orius wide-field side mount CC Digital camera (Gatan Inc., Pleasanton, CA).

RESULTS

Generation of Mice Bearing Col6a3 Exon 16 Deletion—A *Col6a3* exon 16 deletion allele was generated by gene targeting in mouse embryonic stem cells (Fig. 2*A*). The *Col6a3* exon 16 is 54 bp long, encoding 18 amino acids of repeating Gly-*X*-*Y* sequence (Gly-2050–Pro-2067) in the N terminus of the triple-helical domain. Crossing of the heterozygous *Col6a3*$^{+/d16}$ mice generated *Col6a3*$^{+/+}$, *Col6a3*$^{+/d16}$, and *Col6a3*$^{d16/d16}$ in the expected Mendelian ratio (Fig. 2*B*). Total RNA isolated from the *Col6a3*$^{+/+}$, *Col6a3*$^{+/d16}$, and *Col6a3*$^{d16/d16}$ embryonic fibroblasts was analyzed by RT-PCR using primers flanking exon 16 (Fig. 2*C*). The *Col6a3*$^{d16/d16}$ PCR product was smaller than the *Col6a3*$^{+/+}$ counterpart as expected, and DNA sequencing confirmed the in-frame deletion of the 54-bp exon 16 coding sequence in the mutant *Col6a3* mRNA (Fig. 2*D*). The *Col6a3*$^{+/d16}$ fibroblasts expressed comparable levels of the normal and mutant mRNAs (Fig. 2*C*). The results demonstrated that the heterozygous *Col6a3*$^{+/d16}$ mice exhibited a molecular defect similar to the dominant UCMD patients with *COL6A3* exon 16 skipping mutations (23, 25).

Mutant α3(VI) Chain Is Assembled into Collagen VI Tetramers But Not into Microfibrils—To assess whether the mutant α3(VI) chain was synthesized and secreted, fibroblasts from the *Col6a3*$^{+/+}$, *Col6a3*$^{+/d16}$, and *Col6a3*$^{d16/d16}$ mice were metabolically labeled with [^{35}S]cysteine overnight, and collagen VI biosynthesis was analyzed by immunoprecipitation of cell lysate and culture medium with an antibody specific for the α1(VI) chain (26). The anti-α1(VI) antibody should precipitate triple-helical collagen VI molecules containing the α1(VI) chain and also the free α1(VI) chain. When the immunoprecipitated material was analyzed on reduced polyacrylamide gels (Fig. 3*A*), all three collagen VI chains were found in the culture media of the wild type, heterozygous, and homozygous cells. The observation that the anti-α1(VI) antibody could immunoprecipitate all three collagen VI chains in the *Col6a3*$^{d16/d16}$ fibroblasts indicated that the mutant α3(VI) chain with an in-frame deletion of six Gly-*X*-*Y* repeats was synthesized, formed triple-helical collagen VI molecules with the other two chains, and was then secreted extracellularly. In the cell lysates, low levels of all three chains were found in all three genotypes (Fig. 3*A*, *right panel*), indicating that the majority of the triple-helical collagen VI molecules were secreted into the medium. When the immunoprecipitated products were analyzed under non-reduced conditions in composite agarose-polyacrylamide gels, collagen VI tetramers were detected in the culture media and cell lysates of all three genotypes, indicating that triple-helical collagen VI molecules containing the mutant α3(VI) chain could be assembled into tetramers and secreted (Fig. 3*B*). Notably, increased amounts of dimers and a product migrated below the monomers were seen in both the media and cell lysates of the *Col6a3*$^{d16/d16}$ fibroblasts and to a lesser extent in the *Col6a3*$^{+/d16}$ counterparts (Fig. 3*B*, *asterisks*). The product migrated below the normal monomers could represent mutant monomers with alternative disulfide bonding. The result suggested that tetramer assembly from the mutant α3(VI) chain was somewhat compromised, resulting in the accumulation of dimers.

Collagen VI microfibrils are formed by an end-to-end association of the tetramers. To assess collagen VI microfibrillar formation, post-confluent fibroblasts from the *Col6a3*$^{+/+}$, *Col6a3*$^{+/d16}$, and *Col6a3*$^{d16/d16}$ mice were immunostained with antibodies specific for the α3(VI) or α1(VI) chain (26, 27). Collagen VI microfibrils were abundantly deposited in the ECM of the *Col6a3*$^{+/+}$ cells but not in the *Col6a3*$^{+/d16}$ and *Col6a3*$^{d16/d16}$ fibroblasts (Fig. 4). The data indicated that abnormal collagen VI tetramers made up of either the mutant α3(VI) chain exclusively (in *Col6a3*$^{d16/d16}$ cells) or a mixture of normal and mutant α3(VI) chain (in *Col6a3*$^{+/d16}$ cells) could

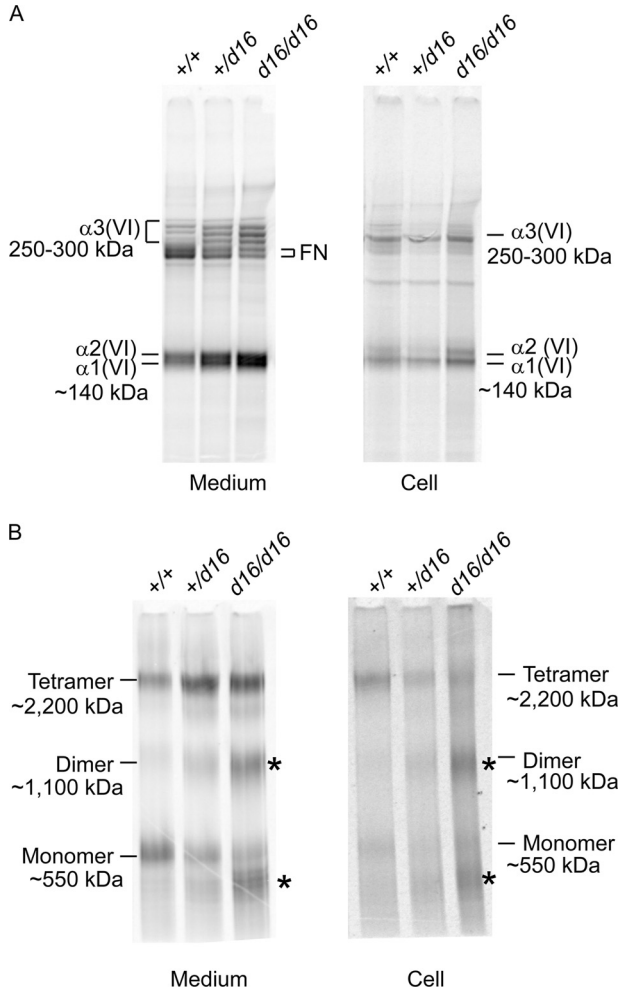

FIGURE 3. **Collagen VI biosynthesis in fibroblasts from the *Col6a3*$^{+/+}$, *Col6a3*$^{+/d16}$, and *Col6a3*$^{d16/d16}$ mice.** Fibroblasts were grown in serum-free medium containing [^{35}S]cysteine overnight. Culture medium and cell lysate were immunoprecipitated with anti-α1(VI) collagen antibody. *A*, immunoprecipitated samples were reduced with 25 mM DTT and separated on 3–8% polyacrylamide gels. Normal and mutant α3(VI) chains were synthesized, assembled into triple-helical collagen VI molecules with the α1(VI) and α2(VI) chains, and secreted. Note that fibronectin (*FN*), which is abundant in the culture medium, was co-precipitated. *B*, samples not treated with DTT were run on composite agarose-polyacrylamide gels. Collagen VI tetramers could be assembled from the mutant α3(VI) chains. Note the accumulation of dimers and the presence of a product below the normal monomers (*asterisks*) in the medium and cell fractions of the two mutant genotypes.

not assemble into long microfibrils. By contrast, fibroblasts from the *Col6a3*$^{+/hm}$ mice (22), which are equivalent to haploinsufficiency in *Col6a3*, deposited a reduced level of collagen VI microfibrils (Fig. 4).

Increased α3(VI) and α1(VI) Immunoreactivity in Mutant Embryos—To determine whether the mutant α3(VI) chain was produced *in vivo*, immunostaining of embryonic tissues during robust collagen VI synthesis at embryonic day 17 (E17) was performed. In coronal sections of the *Col6a3*$^{+/+}$ embryos, both anti-α3(VI) and anti-α1(VI) antibodies showed a fibrous collagen VI staining pattern in the dermis, skeletal muscle, and around the ribs (Fig. 5*A*, *a*, *d*, and *g*). Surprisingly, increased immunoreactivity with both antibodies was observed in the *Col6a3*$^{+/d16}$ and *Col6a3*$^{d16/d16}$ embryos (Fig. 4*A*, *b*, *c*, *e*, and *f*). The strong immunoreactivity detected by the anti-α3(VI) chain antibody in the homozygous tissues indicated that the mutant α3(VI) chain was synthesized and deposited in tissues. High magnification images showed that the immunoreactivity in the mutant tissues did not exhibit the fibrous pattern but instead appeared amorphous (Fig. 5*A*, *h* and *i*). Western blot analysis of tissue extracts from hind limbs of E17 embryos showed that the α1(VI) and α3(VI) chains were increased in the heterozygous and homozygous mutant mice (Fig. 5*B*).

No Change in the Distribution of α3(VI)-like Chains in Mutant Tissues during Development—To determine whether the *Col6a3* mutation resulted in a compensatory up-regulation of the three α3(VI)-like chains, the coronal sections of the E17 embryos were immunostained with chain-specific antibodies (7). The immunoreactivity and distribution of the α4(VI), α5(VI), and α6(VI) chains in the *Col6a3*$^{+/d16}$ and *Col6a3*$^{d16/d16}$ embryos were similar to the wild type embryos. In all three genotypes, the α4(VI) and α5(VI) chains were prominently expressed in the mucosal and submucosal layers of the gut but not detectable in the musculoskeletal tissues (data not shown). The α6(VI) chain was present in the skeletal muscle but absent in the dermis and ribs of all three genotypes, whereas the α3(VI) chain was abundant in all of these tissues (Fig. 6*A*). In addition, the α6(VI) chain was found in diaphragm but not in lung (except pleura) of all three genotypes (Fig. 6*B*), unlike the prominent expression of α3(VI) chain in lung tissue (not shown). Collagen VI is abundant in tendon tissue. Immunoreactivity of the α6(VI) chain in tendon was compared using 2-week-old mouse tails. Again, no difference was observed among the three

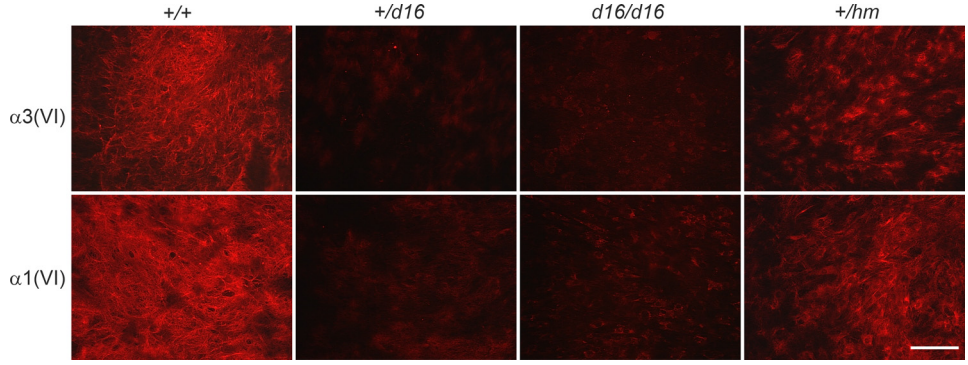

FIGURE 4. **Immunostaining of collagen VI microfibrils deposited by the *Col6a3*$^{+/+}$, *Col6a3*$^{+/d16}$, *Col6a3*$^{d16/d16}$, and *Col6a3*$^{+/hm}$ fibroblasts.** Cells were grown for 4 days post-confluence and then immunostained with antibodies specific for the α3(VI) or α1(VI) chain. Microfibrils were barely detectable in the *Col6a3*$^{+/d16}$ and *Col6a3*$^{d16/d16}$ fibroblasts. The *Col6a3*$^{+/hm}$ fibroblasts deposited reduced amounts of collagen VI microfibrils. *Magnification bar* = 50 μm.

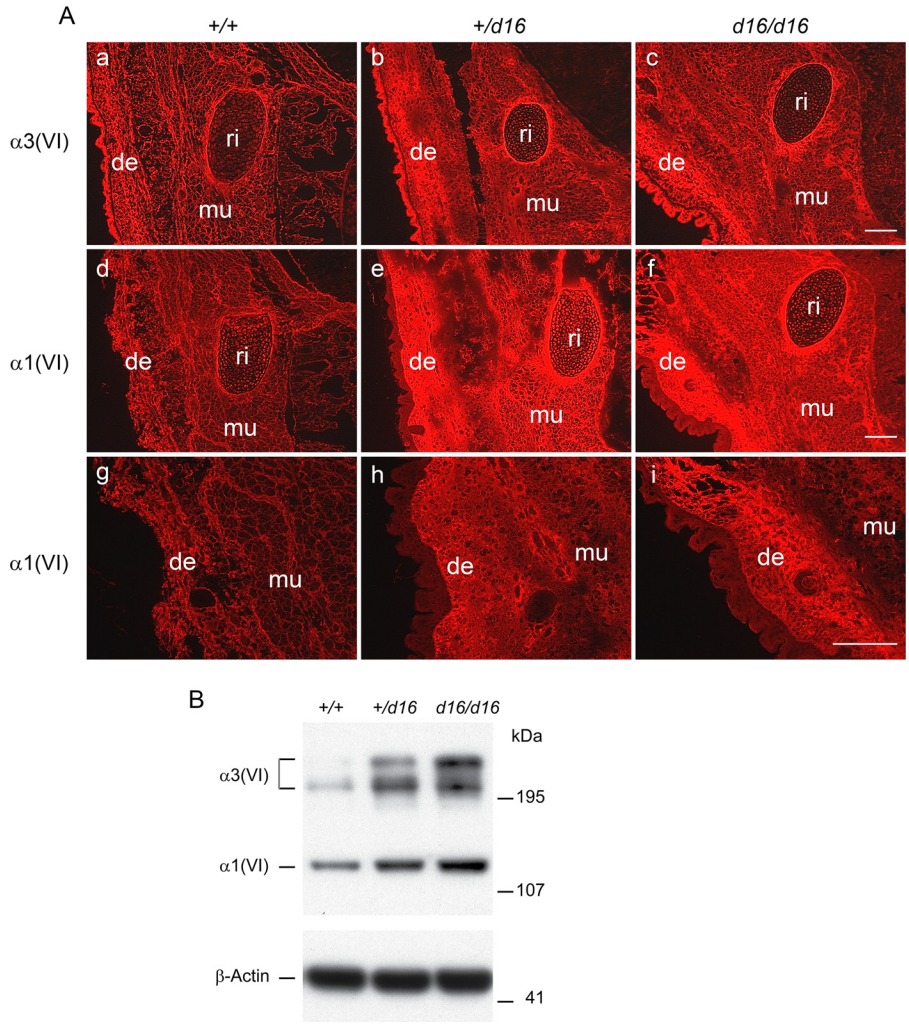

FIGURE 5. **Increased collagen VI immunoreactivity in mutant mice during embryonic development.** *A*, immunostaining of coronal sections of embryonic day 17 *Col6a3*$^{+/+}$, *Col6a3*$^{+/d16}$, and *Col6a3*$^{d16/d16}$ littermates. Cryosections were stained with antibodies specific for the α3(VI) (*a–c*) or α1(VI) chain (*d–i*). Increased immunoreactivities of both chains were seen in the *Col6a3*$^{+/d16}$ and *Col6a3*$^{d16/d16}$ embryos. High magnification images (*g–i*) show fibrous collagen VI staining of the *Col6a3*$^{+/+}$ embryo but amorphous staining of the *Col6a3*$^{+/d16}$ and *Col6a3*$^{d16/d16}$ embryos. *de*, dermis; *ri*, rib; *mu*, muscle. *Magnification bars* = 50 μm. *B*, Western blot analysis of α3(VI) and α1(VI) collagen chain levels in tissue extracts from E17 limbs. Increased levels of both chains were found in the *Col6a3*$^{+/d16}$ and *Col6a3*$^{d16/d16}$ limbs. Note that two α3(VI) bands were detected, and the lower band corresponded to a processing product lacking part of the C-terminal globular domain.

genotypes (Fig. 6*C*). The α6(VI) chain was expressed only in tendon sheaths but not within tendon fascicles, whereas the α3(VI) chain was robustly present in the tendon fascicles and less prominent in the tendon sheaths. In addition, the α6(VI) chain was absent in the nerves and vertebrae, in contrast to the α3(VI) chain.

Reduced α3(VI) and α1(VI) Immunoreactivity in Postnatal Col6a3$^{+/d16}$ *and Col6a3*$^{d16/d16}$ *Muscles*—Both homozygous and heterozygous mutant mice had no obvious abnormal phenotypes. They were fertile and had normal life spans, surviving up to 2 years of age. To assess collagen VI protein expression in skeletal muscles of the postnatal mutant mice, limb and diaphragm muscles from young mice (2–6 weeks) were examined by immunohistochemistry using the antibodies against the α1(VI) and α3(VI) chains. As shown in the representative images of quadriceps muscles from 1-month-old mice (Fig. 7), the α3(VI) and α1(VI) immunoreactivities were somewhat decreased in the *Col6a3*$^{+/d16}$ muscle. In the *Col6a3*$^{d16/d16}$ muscles, whereas the α3(VI) immunoreactivity was substantially reduced compared with the *Col6a3*$^{+/d16}$ muscle, the decrease in the α1(VI) immunoreactivity between the two mutant genotypes was less visible. The data suggested that 1) the abnormal collagen VI protein present at high levels at embryonic stages (Fig. 5) were unstable and prone to degradation over time when the growth slowed down, and 2) collagen VI molecules with a chain composition other than α1(VI)α2(VI)α3(VI) might be present. To determine whether the three α3(VI)-like α chains could substitute for the α3(VI) chain and assemble with the α1(VI) and α2(VI) chains in muscle, immunostaining with antibodies specific for the α4(VI), α5(VI), and α6(VI) chains was performed. The α6(VI) chain was found at comparable levels in all three genotypes (Fig. 7), whereas immunoreactivity with the α4(VI) or α5(VI) chains was not detectable (data not shown). The results suggested that the α6(VI) chain could form triple-helical collagen VI molecules with the α1(VI) and α2(VI) chains in muscle, but there was no significant compensatory up-regulation of the α6(VI) chain in the two mutant genotypes.

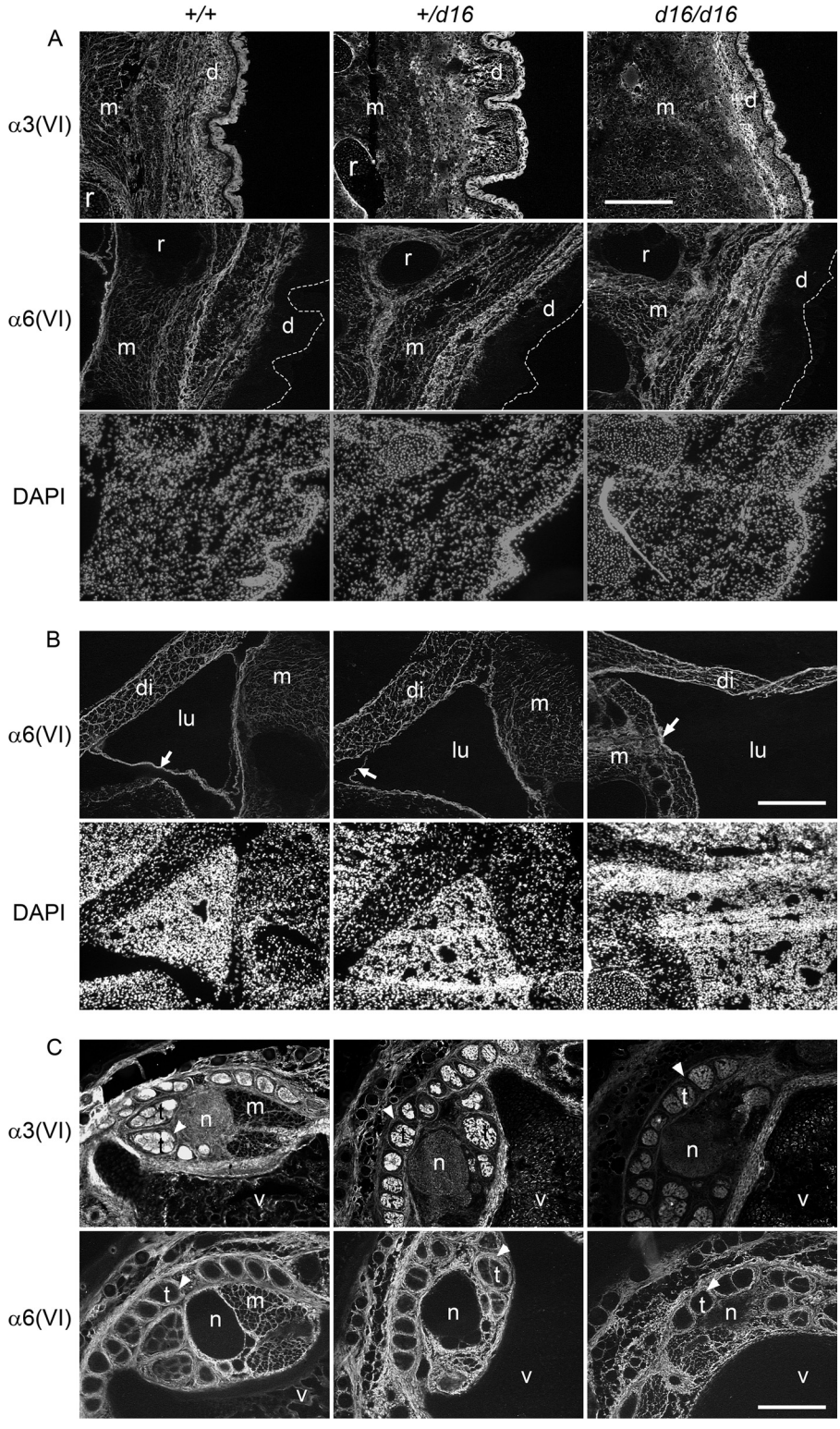

FIGURE 6. **Distribution of the α6(VI) collagen chain is not altered in the mutant mice during development.** Cryosections were immunostained with antibodies against α3(VI) and α6(VI) chains and treated with DAPI to visualize nuclei. *A* and *B*, coronal sections of E17 *Col6a3*$^{+/+}$, *Col6a3*$^{+/d16}$, and *Col6a3*$^{d16/d16}$ embryos. *A*, the α3(VI) chain is present in the dermis (*d*), ribs (*r*), and skeletal muscle (*m*). The α6(VI) chain is present in skeletal muscle but not in ribs and dermis of all three genotypes. DAPI images corresponding to the α6(VI) stainings are shown in the *third row*. *B*, the α6(VI) chain is present in diaphragm (*di*), skeletal muscle (*m*), pleura (*arrows*) but not in lung (*lu*) of all three genotypes. DAPI images are shown in the *second row*. *C*, cross-sections of 2-week mouse tails. The α6(VI) chain is present in tendon sheath (*arrowheads*) and muscle (*m*) but not in tendon fascicles (*t*), nerve (*n*), and vertebrae (*v*). The α3(VI) chain is present in tendon fascicles, muscle, nerve, and vertebrae. *Magnification bars* = 50 μm.

Col6a3$^{+/d16}$ *and Col6a3*$^{d16/d16}$ *Mice Display Myopathic Histology*—Limb and diaphragm muscles from the *Col6a3*$^{+/+}$, *Col6a3*$^{+/d16}$, and *Col6a3*$^{d16/d16}$ mice at different ages were examined by histology. Variation in muscle fiber size, myofibers with centrally located nuclei, and increased endomysial connective tissue were readily seen in the *Col6a3*$^{+/d16}$ and

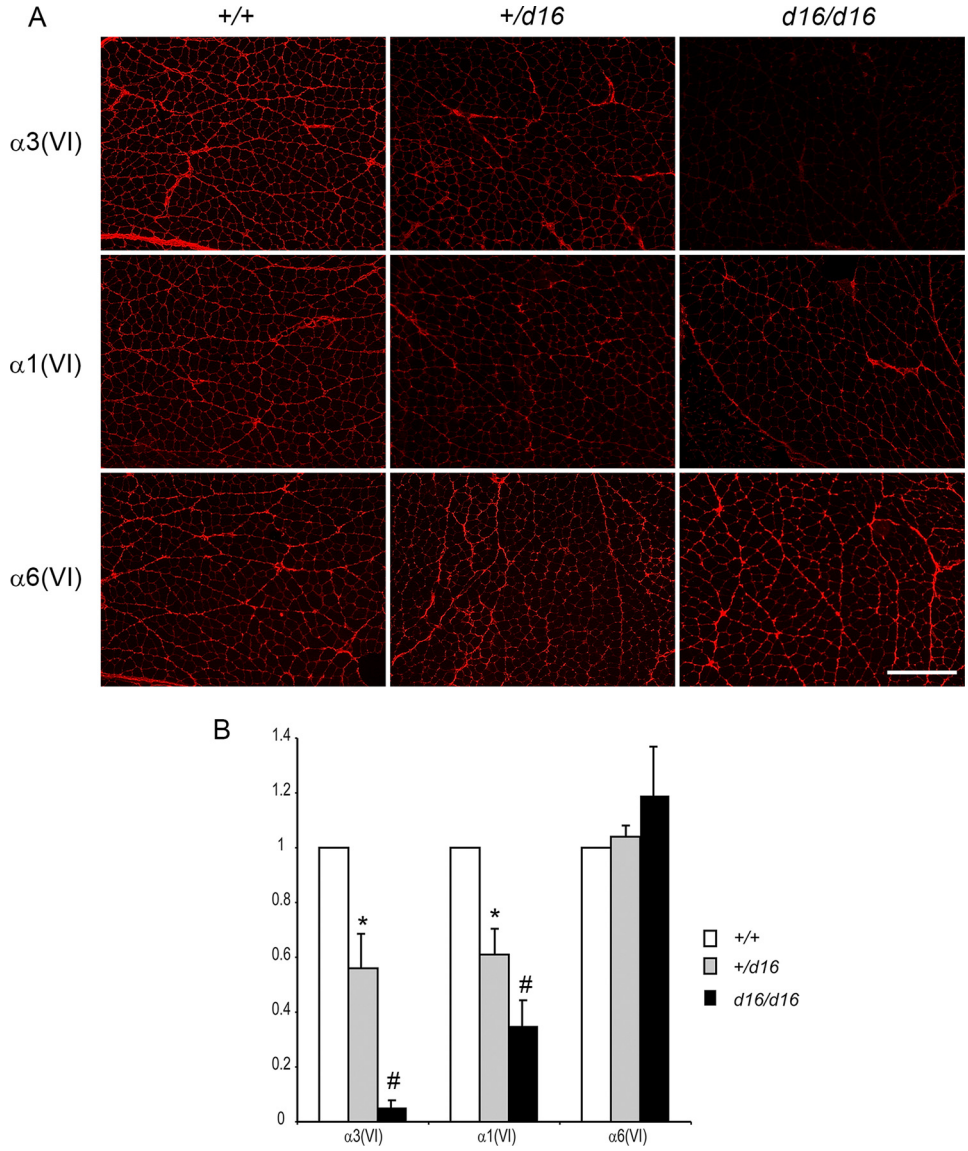

FIGURE 7. **Immunoreactivity of collagen VI chains in skeletal muscles of 1-month-old *Col6a3*$^{+/+}$, *Col6a3*$^{+/d16}$ and *Col6a3*$^{d16/d16}$ mice.** *A*, representative images of cryosections from quadriceps muscles immunostained with polyclonal antibodies specific for the α3(VI), α1(VI), and α6(VI) collagen chains. *Magnification bar* = 50 μm. *B*, relative fluorescence intensity of images from three sets of independent samples. The intensity of the *Col6a3*$^{+/+}$ sample was set as 1.00. Values of the two mutant genotypes were mean ± S.D. (*error bars*). *, $p < 0.05$ between *Col6a3*$^{+/+}$ and *Col6a3*$^{+/d16}$; #, $p < 0.05$ between *Col6a3*$^{+/+}$ and *Col6a3*$^{d16/d16}$. The immunoreactivities of α3(VI) and α1(VI) chains were reduced in the *Col6a3*$^{+/d16}$ and *Col6a3*$^{d16/d16}$ muscles. In the *Col6a3*$^{d16/d16}$ muscle, the α1(VI) chain was readily seen, but the α3(VI) chain was barely detectable. The α6(VI) immunoreactivity was similar in all three genotypes.

Col6a3$^{d16/d16}$ mice at age 6 months (Fig. 8*A*). The muscle abnormalities were already noticeable in younger mice. As shown in Fig. 8*B*, the percentages of myofibers with central nuclei in the *Col6a3*$^{+/d16}$ and *Col6a3*$^{d16/d16}$ mice were higher than the wild type controls at ages 1, 3, 6, and 12 months. Measurement of single muscle fiber areas in quadriceps muscles from the 6-month-old *Col6a3*$^{+/d16}$ and *Col6a3*$^{d16/d16}$ mice showed the wide distribution in muscle fiber sizes (Fig. 8*C*). There were more small and large fibers in the mutant mice compared with the wild type animals. The results indicated that both *Col6a3*$^{+/d16}$ and *Col6a3*$^{d16/d16}$ exhibited progressive myopathic histopathology.

ECM Changes in the Col6a3$^{+/d16}$ *and Col6a3*$^{d16/d16}$ *Muscles*—Histological analysis of muscles from 6-month-old *Col6a3*$^{+/d16}$ and *Col6a3*$^{d16/d16}$ mice above suggested substantial increases in endomysial matrix. Therefore, immunostaining with selected ECM molecules was performed. In quadriceps muscles from 6-month-old mice, the α3(VI) and α1(VI) immunoreactivities were decreased in the *Col6a3*$^{+/d16}$ and *Col6a3*$^{d16/d16}$ muscles compared with the wild type counterpart (Fig. 9), similar to the findings of the young mice described above (Fig. 7). Among the α3(VI)-like chains, the α4(VI) chain was not detected in the muscles of all three genotypes as expected (not shown). However, immunoreactivities of the α5(VI) and α6(VI) chains were both increased around some myofibers of the two mutant genotypes, unlike the observations in the young mice. The staining patterns of the α5(VI) and α6(VI) resembled the immunoreactivities of collagen type I, a principal marker for fibrosis, and periostin, a profibrotic ECM protein (Fig. 9) (32). Immunoreactivity of tenascin-X, an ECM protein we previously found to be up-regulated in the *Col6a3*$^{hm/hm}$ mice (22), was also increased in the *Col6a3*$^{+/d16}$ and *Col6a3*$^{d16/d16}$ muscles.

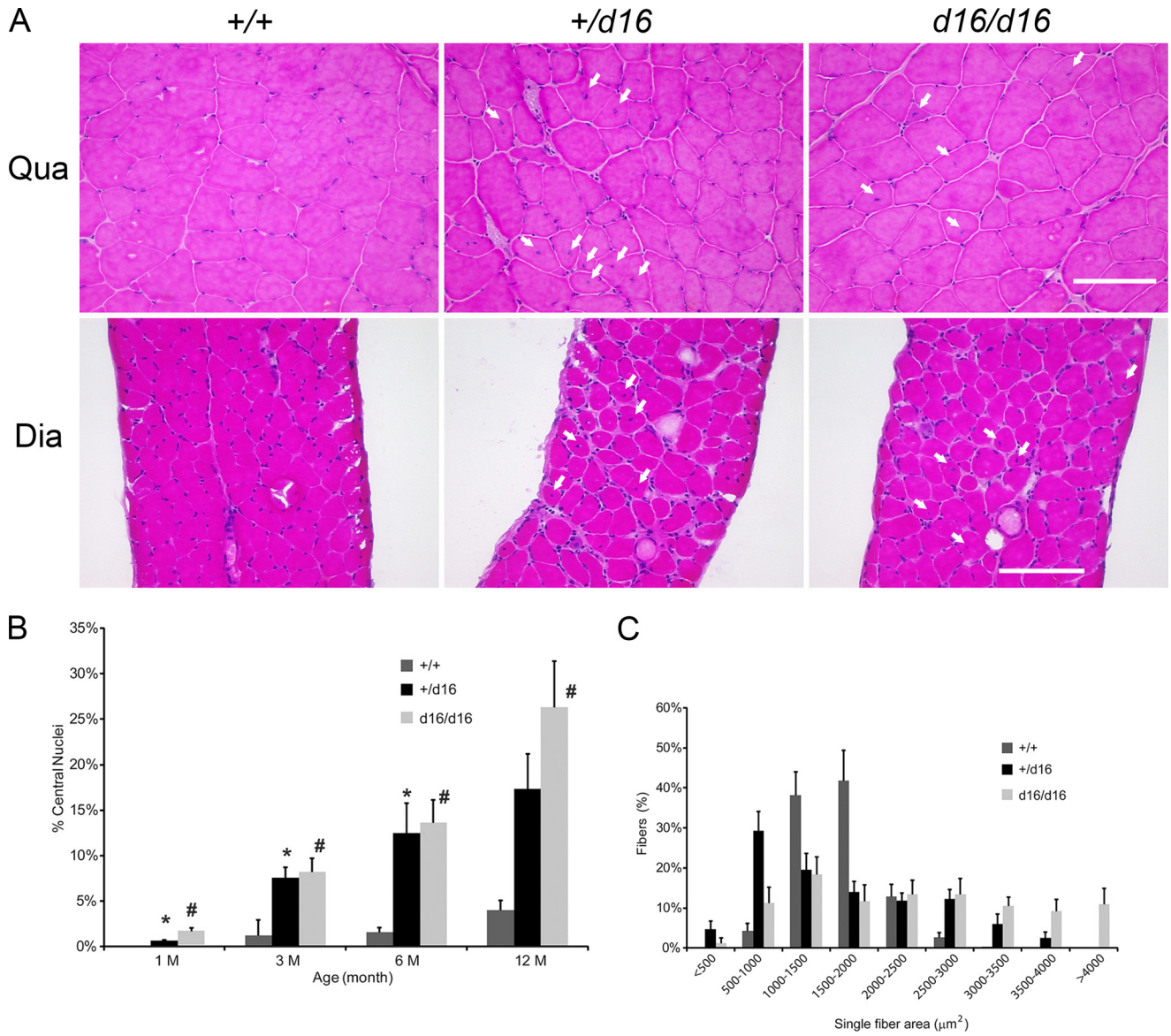

FIGURE 8. **Histological analysis of the *Col6a3*$^{+/+}$, *Col6a3*$^{+/d16}$, and *Col6a3*$^{d16/d16}$ muscles.** *A*, representative images of quadriceps (*Qua*) and diaphragm (*Dia*) muscles from 6-month-old *Col6a3*$^{+/+}$, *Col6a3*$^{+/d16}$, and *Col6a3*$^{d16/d16}$ mice. Cryosections were stained with hematoxylin and eosin. Wide variations in muscle fiber size and many centrally localized nuclei (*arrows*) were found in heterozygous and homozygous mutant mice. *Magnification bars* = 50 μm. *B*, quantification of the percentage of muscle fibers with centrally located nuclei. Quadriceps muscles from 1-, 3-, 6-, and 12-month old mice of three genotypes were analyzed. *C*, distribution of single fiber areas in quadriceps muscles from 6-month-old mice. Data in *panels B* and *C* were from four muscles per group and are expressed as mean ± S.D. (*error bars*). *, $p < 0.05$ between *Col6a3*$^{+/+}$and *Col6a3*$^{+/d16}$; #, $p < 0.05$ between *Col6a3*$^{+/+}$and *Col6a3*$^{d16/d16}$.

Ultrastructural Alterations in the Col6a3$^{+/d16}$ *and Col6a3*$^{d16/d16}$ *Muscles*—A distinct pathological finding of the *Col6a1* null mice is the morphological alteration of mitochondria and sarcoplasmic reticulum in the skeletal muscle (33). Therefore, transmission electron microscopy of gastrocnemius muscles from 1-month-old mice was performed. The analyses showed ultrastructural changes in the mitochondria and sarcoplasmic reticulum of the *Col6a3*$^{+/d16}$ and *Col6a3*$^{d16/d16}$ mice. A substantial proportion of the mitochondria in the two mutant genotypes were enlarged and irregularly shaped, and the sarcoplasmic reticula were distended (Fig. 10*A*). In addition, collagen fibrils in the endomysial connective tissue of the two mutant genotypes appeared disorganized (Fig. 10*B*).

Abnormal Collagen Fibrils in the Col6a3$^{+/d16}$ *and Col6a3*$^{d16/d16}$ *Tendons*—Patients affected with collagen VI disorders have tendon defects. Therefore, FDL and Achilles tendons from 1-month-old mice of the three genotypes were assessed by transmission electron microscopy. Cross-sectional images of both types of tendons revealed abnormal collagen fibril morphology in the mutant mice (Fig. 11). Collagen fibrils in the *Col6a3*$^{+/+}$ tendons were densely packed and composed of large and small fibrils with uniform circular outlines. By contrast, collagen fibrils in the *Col6a3*$^{+/d16}$ and *Col6a3*$^{d16/d16}$ tendons were less organized and sparse in some areas. Moreover, there were unusually large fibrils with cauliflower-like fibril contours and many small diameter fibrils. Abnormal collagen fibrils were mostly located in the pericellular regions (Fig. 11) and less

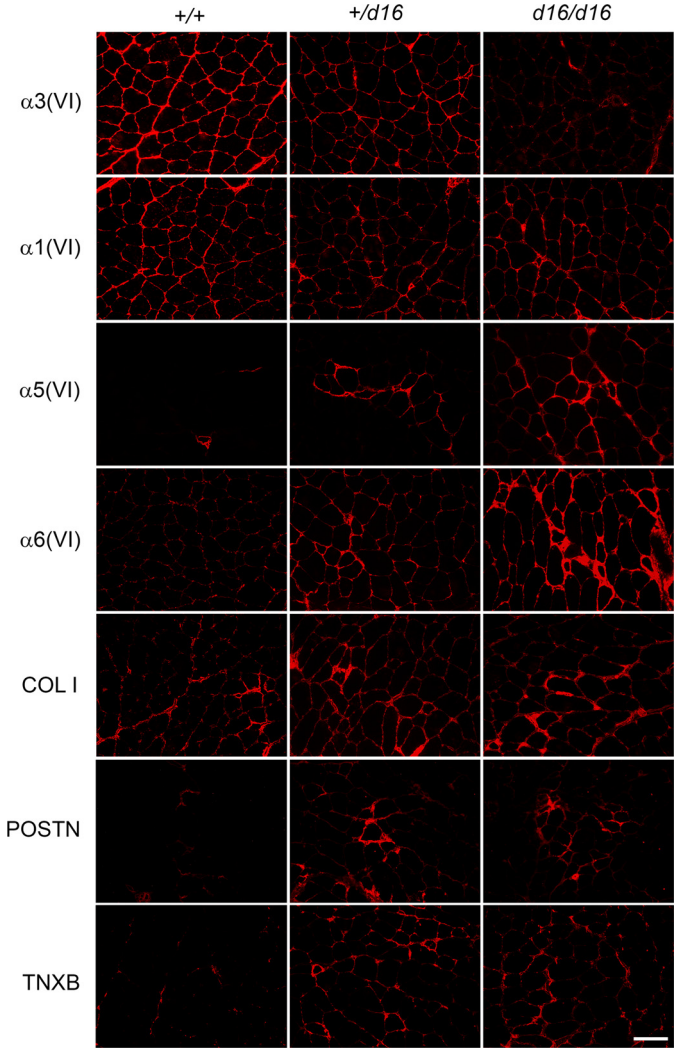

FIGURE 9. **Increased immunoreactivities of selected ECM proteins in skeletal muscles of 6-month-old mutant mice.** Cryosections of quadricep muscles from *Col6a3*$^{+/+}$, *Col6a3*$^{+/d16}$, and *Col6a3*$^{d16/d16}$ mice aged 6 months were immunostained with polyclonal antibodies specific for collagen VI (α3, α1, α5, and α6 chains), collagen type I (*COL I*), periostin (*POSTN*), and tenascin-X (*TNXB*). Three mice from each genotype were analyzed.

abundant in areas distant from the cells (not shown). In addition, tenocyte organization was disrupted in the mutant genotypes with cellular processes defining extracellular domains containing collagen fiber poorly organized. The abnormal cellular organization is consistent with altered cell-matrix interactions in the presence of mutant collagen VI.

Muscle Function of the Col6a3$^{+/d16}$ *Mice Is Compromised*—Histological and ultrastructural analyses indicated that the *Col6a3*$^{+/d16}$ mice displayed notable muscle abnormalities. To further evaluable whether the *Col6a3*$^{+/d16}$ mouse is a suitable animal model for dominant UCMD, physiological assessment of the *Col6a3*$^{+/d16}$ muscles at ages 3 and 8 months was performed. The *Col6a3*$^{+/d16}$ mice showed significantly reduced muscle contractile function at age 8 months (Table 1) but not at 3 months (data not shown). In the 8-month-old *Col6a3*$^{+/d16}$ mice, growth and weight of some muscle groups were reduced (Table 1). EDL muscles from the *Col6a3*$^{+/d16}$ and control mice were used to measure peak force. Twitch contraction force of the EDL muscle from the *Col6a3*$^{+/d16}$ was significantly

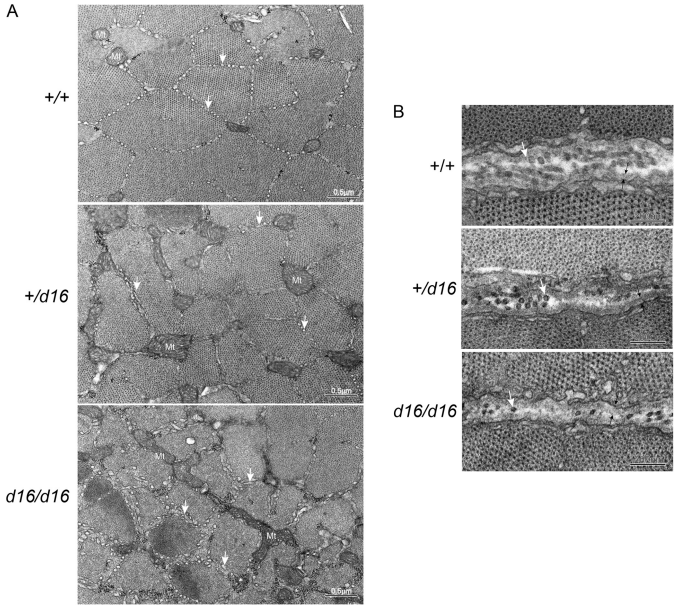

FIGURE 10. **Ultrastructural analysis of the *Col6a3*$^{+/+}$, *Col6a3*$^{+/d16}$, and *Col6a3*$^{d16/d16}$ muscles.** Gastrocnemius muscles from 1-month-old mice were examined by transmission electron microscopy. *A*, mitochondria (*Mt*) and sarcoplasmic reticulum (*arrows*) in the *Col6a3*$^{+/d16}$ and *Col6a3*$^{d16/d16}$ muscles were dilated. *Magnification bars* = 0.5 μm. *B*, endomysium in the *Col6a3*$^{+/d16}$ and *Col6a3*$^{d16/d16}$ muscles appeared less structured with fewer collagen fibrils (*white arrows*). In homozygous mice, lamina densa (between *black arrows*) appeared to be more electron lucent and detached from the sarcolemma in some regions. *Magnification bars* = 200 nm.

reduced. Tetanus contraction force of the *Col6a3*$^{+/d16}$ EDL muscle also was decreased, but statistical significance was not reached. No significant differences were observed in ECC-induced force decrement and cross-sectional area of the EDL muscles.

DISCUSSION

Skipping of *COL6A3* exon 16, due to splice site mutations or small deletion, is the most common molecular defect in dominant UCMD patients (11, 13, 23, 25). In this study we deleted exon 16 and its flanking sequence in the mouse *Col6a3* gene by gene targeting. We show that the heterozygous mutant mice, *Col6a3*$^{+/d16}$, produce comparable amounts of the normal and exon 16-deleted *Col6a3* mRNA similar to those patients with the heterozygous exon 16 skipping mutations (23, 25). The *Col6a3*$^{+/d16}$ mice thus represent a mouse model of dominant UCMD.

The deletion of *Col6a3* exon 16 removes 6 Gly-*X*-*Y* repeats in the N terminus of the triple-helical domain of the α3(VI) collagen chain (amino acids 16–33 counting from the beginning of the triple-helical domain) but preserves the unique cysteine residue (amino acid 50) essential for collagen VI tetramer assembly (Fig. 1, *A* and *B*). Current evidence suggests that folding of the three collagen VI chains into triple-helical molecules proceeds from the C to N terminus, similar to collagen type I (18, 34). Therefore, the mutant α3(VI) chain with a small in-frame deletion in the N terminus should be able to assemble into collagen VI triple-helical monomers. Examination of the amino acid sequence indicates that the deleted Gly-*X*-*Y* repeats are of low triple-helix propensity (35) (Fig. 2*D*). Therefore, the N terminus of the normal collagen VI triple helix is likely to be

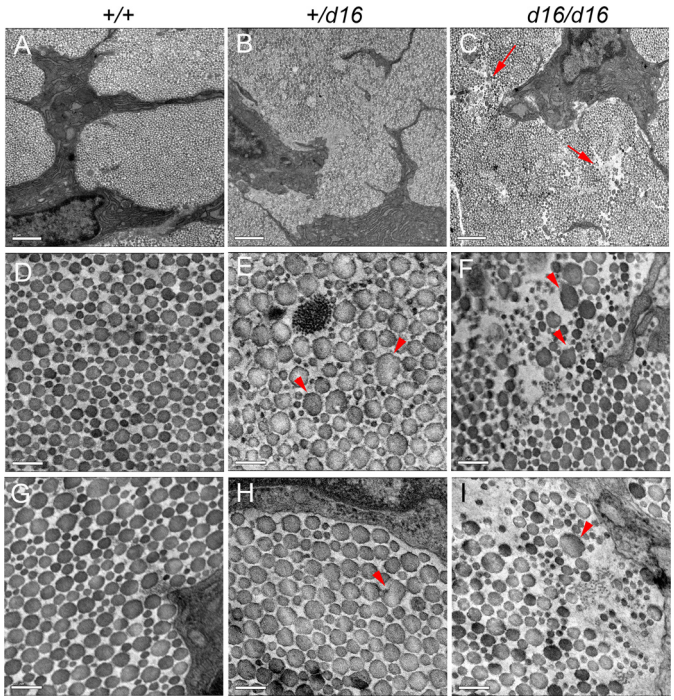

FIGURE 11. **Ultrastructural analysis of the *Col6a3*$^{+/+}$, *Col6a3*$^{+/d16}$, and *Col6a3*$^{d16/d16}$ tendons.** Flexor FDL and Achilles tendons of 1-month-old *Col6a3*$^{+/+}$, *Col6a3*$^{+/d16}$, and *Col6a3*$^{d16/d16}$ mice were examined by electron microscopy. *A–C*, FDL tendons at low magnification (*bars* = 1 μm). Collagen fibrils in the two mutant genotypes were disorganized. In the homozygous mutant mice, collagen fibrils were sparse in some regions (*arrows*). In addition, tenocyte organization was disrupted in the mutant genotypes with cellular processes defining extracellular domains containing collagen fiber poorly organized. *D–F*, FDL tendons at high magnification (*bars* = 200 nm). Abnormally large collagen fibrils with rough contours (*arrowheads*) and many small diameter fibrils were observed in the two mutant genotypes. *G–I*, Achilles tendons. Collagen fibrils in the two mutant genotypes showed similar ultrastructural defects as the FDL tendons. *Magnification bars* = 200 nm.

TABLE 1

Morphometric and muscle contractile properties of the *Col6a3*$^{+/d16}$ mice

CSA, cross-sectional area. mN, millinewtons. Results are presented as the mean ± S.D.

Genotype Number of mice Number of muscles	+/+ $n = 5$ $n_{muscle} = 10$	+/d16 $n = 6$ $n_{muscle} = 11$
Body weight (g)	25.6 ± 1.14	22.8 ± 1.60[a]
Muscle weight (mg)		
EDL	10.8 ± 0.68	9.8 ± 0.82
Soleus	8.4 ± 1.03	7.8 ± 1.08
Gastrocnemius	115.3 ± 16.94	97.4 ± 15.49[a]
Tibialis anterior	38.7 ± 3.44	36.1 ± 2.46
Quadriceps	135.6 ± 19.61	113.3 ± 16.73[a]
Diaphragm	67.4 ± 12.1	53.6 ± 6.60
EDL contractile properties		
Twitch		
Absolute force (mN)	102.2 ± 19.64	67.1 ± 22.04[a]
Specific force (mN/mm^2)	55.9 ± 12.66	42.9 ± 10.98[a]
Specific force (mN/mg)	9.6 ± 2.16	7.0 ± 2.18[a]
Tetanus		
Absolute force (mN)	397.5 ± 94.77	306.7 ± 113.51
Specific force (mN/mm^2)	217.0 ± 56.36	201.1 ± 84.71
Specific force (mN/mg)	37.3 ± 10.10	32.3 ± 12.67
ECC force drop 1–5 (%)	18.8 ± 11.28	16.9 ± 11.31
EDL Length (mm)	12.3 ± 0.66	13.3 ± 1.34
CSA (mm^2) by Brooks-Faulkner	1.8 ± 0.14	1.6 ± 0.26

[a] Statistically significant between wild type and heterozygous mutant ($p < 0.05$).

a relatively unstable region. When a small in-frame deletion is present in the N-terminal triple-helical region of the α3(VI) chain, it is possible that the triple-helix folding continues upon reaching the deleted region, although out of register, until the end of the α3(VI) collagenous domain, thereby leaving overhangs of unfolded α1(VI) and α2(VI) chains. Alternatively, the triple helix folding could stop at the deleted region, leaving all three chains unfolded. In either case, the N terminus of the triple helix would be misfolded. However, dimers and tetramers are expected to be assembled, as the single cysteines in the three chains essential for oligomer assembly/stabilization are preserved (Fig. 1*B*). Biosynthetic studies of mouse fibroblasts indeed confirm that monomers, dimers, and tetramers are formed when either a half or all of the α3(VI) chains contain the deletion in the heterozygous or homozygous cells, respectively (Fig. 3, *A* and *B*). Theoretically, in the heterozygous cells, 15 out of 16 tetramers contain at least one mutant α3(VI) chain and the abnormal tetramers with defective N termini are unable to assemble end-to-end into microfibrils (18) (Fig. 1*C*). The effects of the N-terminal mutations are further amplified during the formation of long microfibrils as this process requires the association of multiple tetramers via their N termini. Consistent with this proposition, we show that collagen VI microfibrils are barely detectable in both heterozygous and homozygous fibroblasts (Fig. 4). Given that collagen VI microfibrils are readily seen in fibroblasts from mice heterozygous for the nonfunctional *Col6a3* mutant allele (*Col6a3*$^{+/hm}$, Fig. 4), the results demonstrate that heterozygous exon 16 deletion in *Col6a3* exerts a dominant negative effect on collagen VI microfibrillar assembly. In the homozygous cells, all of the tetramers are defective and cannot assemble microfibils. Therefore, the *Col6a3*$^{d16/d16}$ mice should be equivalent to the collagen VI null mice reported previously (21).

An unexpected finding is that high levels of the α1(VI) and α3(VI) immunoreactivity are present in embryonic tissues of both heterozygous and homozygous mutant mice. The nonfibrous appearance of the immunostaining in the mutant mice suggests that collagen VI microfibrils are not assembled. The observed increase in immunoreactivity may result from accumulation of unassembled collagen VI tetramers in the interstitial matrix. This interpretation is supported by results from Western blot and biosynthetic studies. In tissue extracts of the limbs, higher levels of the collagen VI chains were detected in the mutant mice by Western blotting (Fig. 5). Biosynthetic studies with embryonic fibroblasts demonstrate that higher levels of tetramers are present in the culture media of the two mutant genotypes compared with the wild type counterpart (Fig. 3*B*). In the wild type mice, the majority of the newly synthesized tetramers presumably have been assembled into collagen VI microfibrils, which are more difficult to extract from tissue. The unassembled collagen VI tetramers accumulated during embryonic stages most likely are subject to degradation over time when growth rate slows down, as collagen VI immunoreactivity is reduced in the postnatal skeletal muscles from heterozygous and homozygous mutant mice (Fig. 7).

Our studies show that the lack of normal α3(VI) chain in the mutant mice does not lead to a compensatory up-regulation of the three α3(VI)-like chains in skeletal muscle and other organs during development (Fig. 6). This is most likely attributed to the low abundance and highly restricted tissue distribution pat-

terns of the three α3(VI)-like chains. Previous studies have shown that the α4(VI) chain is not, and the α5(VI) chain is only weakly expressed in the skeletal muscle (7). The α6(VI) chain is present in the endomysium and perimysium of fetal and adult skeletal muscle, but its expression level is much lower than the α3(VI) chain (6, 7). Our studies extend these previous findings and demonstrate the distinctively restricted expression of the α6(VI) chain in the musculoskeletal tissue as opposed to the ubiquitous distribution of the α3(VI) chain. The absence of the α6(VI) chain in tendon proper, bone/cartilage, and dermis suggests that the *Col6a3* and *Col6a6* genes are independently regulated and implies that *COL6A6* mutations, if any, would result in a disease manifestation distinct from UCMD. On the other hand, we found increased immunoreactivities of the α5(VI) and α6(VI) chains in a subset of muscle fibers in mutant mice at age 6 months, a stage when muscle fibrosis has developed in the mutant mice. Our results partially agree with a recent finding in patients with Duchenne muscular dystrophy, demonstrating that α6(VI), but not α5(VI), chain is up-regulated in fibrotic areas of muscle biopsies (36). Together, these observations support an association of the α5(VI) and α6(VI) chains with muscle fibrosis.

Like mouse models for Duchenne muscular dystrophy (*mdx* mouse) and for recessive UCMD (*Col6a1* null and *Col6a3*$^{hm/hm}$ mice), the *Col6a3*$^{+/d16}$ mice display much milder gross and myopathic phenotypes compared with patients with heterozygous exon 16 skipping mutations. The milder muscle phenotype in *mdx* mice compared with human patients is thought to be related at least in part to the intrinsic difference in muscle regeneration capacity between humans and mice (37). Even though the *Col6a3*$^{+/d16}$ mice have mild phenotypes, we show that the myopathic pathology, such as changes in muscle fiber size and percentage of muscle fibers with central nuclei, can be detected in young mice. Moreover, dilated sarcoplasmic reticulum and enlarged mitochondria are apparent in muscles from both mutant genotypes at age 1 month. The histological and ultrastructural abnormalities of the *Col6a3*$^{+/d16}$ muscles can be used to follow disease progression.

Significant decrease in muscle contractile function can be seen when the *Col6a3*$^{+/d16}$ mice reach age 8 months but not in young adult mice at 3 months. The reduction in muscle force was overall proportional to the degree of reduction in muscle growth and muscle weight (EDL and quadriceps). ECC force decrement is considered to be a hallmark of Duchenne muscular dystrophy (29) and, therefore, is not expected to be observed in mouse models other than the *mdx* mice. We have previously shown that the *Col6a3*$^{hm/hm}$ mice display reduced muscle contractile forces after twitch and tetanic stimulation at age 4 months (22). In UCMD patients, whereas recessive mutations causing an absence of collagen VI almost invariantly display an "early-severe (never acquired ambulation)" phenotype, dominant mutations causing skipping of *COL6A3* exon 16 result in both early-severe and "moderate-progressive (loss of ambulation at a mean age of 10 years)" manifestations (13). These observations suggest that dominant exon skipping mutation may result in a somewhat less severe phenotype compared with recessive mutations that lead to mRNA decay and that modifier genes likely contribute to the phenotypic variations of dominant exon skipping mutations. Consistent with this suggestion is the finding that the *Col6a3*$^{d16/d16}$ mice, which are equivalent to collagen VI null mice, show more pronounced muscle and tendon histopathology than the *Col6a3*$^{+/d16}$ mice. Our studies show that the *Col6a3*$^{+/d16}$ mice exhibit ultrastructural abnormalities in mitochondria and sarcoplasmic reticulum similar to the *Col6a1* null mice and patients carrying collagen VI mutations (33, 38). Whether the *Col6a3*$^{+/d16}$ mice display mitochondrial transition pore defects that can be reversed by cyclosporine A treatment remains to be investigated (33, 39). Nevertheless, the *Col6a3*$^{+/d16}$ mice are ideally suited for testing allele-specific silencing strategies to treat dominant collagen VI disorders. For instance, an antisense oligoribonucleotide has been successfully employed to deplete mutant *COL6A2* mRNA in fibroblasts from a UCMD patient with a heterozygous *COL6A2* mutation (40).

Histological and ultrastructural analyses indicate alteration of the endomysium in the mutant mice, suggesting that collagen VI plays a role in modulating muscle ECM. Immunohistochemistry studies (Fig. 9) show increased expression of ECM proteins that are associated with tissue fibrosis (collagen I and periostin) or regulate collagen fibrillogenesis (tenascin-X, periostin) (32, 41). The observed changes in ECM composition likely influence the mechanical properties of the endomysial connective tissue and thereby alter cellular activities. Consistent with this notion is the recent finding that muscles from the *Col6a1* null mice display reduced stiffness, which leads to compromised activity of muscle satellite cells (42). Mutations of tenascin-X underlie a form of Ehlers-Danlos syndrome, characterized by joint hypermobility and skin laxity similar to patients with collagen VI muscle disorders (43, 44). Fibroblasts from tenascin-X-deficient mice have reduced levels of collagen VI mRNA and protein (45), suggesting coordinate regulation of collagen VI and tenascin-X. Interestingly, mice lacking tenascin-X exhibit mild myopathy (46). Periostin is a matricellular protein capable of directly interacting with collagen I and regulating collagen I fibrillogenesis (32). Periostin is up-regulated in the δ-sarcoglycan null mouse model of muscular dystrophy, and its absence markedly improves the skeletal muscle abnormalities of the mutant mice (47). It is unclear whether the increases in these ECM proteins are compensatory responses to the deficiency of collagen VI. Nevertheless, these proteins have potential to serve as biomarkers for disease progression or targets for developing therapies.

The FDR and Achilles tendons of both *Col6a3*$^{+/d16}$ and *Col6a3*$^{d16/d16}$ mice exhibit abnormalities in collagen fibril structure, cellular shape, and tenocyte processes defining extracellular domains, in accordance with previous findings of FDR tendons in the *Col6a1* null and *Col6a3*$^{hm/hm}$ mice (22, 31). In tendons, collagen VI is concentrated in the pericellular region, likely through direct binding to cell surface receptors on tendon fibroblasts (48). Collagen VI also interacts with small proteoglycans, including decorin and biglycan, which are known to regulate collagen I fibrillogenesis (49, 50). Deficiency in collagen VI alters the pericellular matrix network and thereby may also modulate the cellular activity. Indeed, a small increase in the MMP-2 activity has been found in tendons from the *Col6a1* null mice (31). Though the molecular mechanism by which

collagen VI regulates collagen fibril morphology remains unclear, the ability of collagen VI to mediate cell-matrix and matrix-matrix interactions likely plays a central role.

In summary, we have generated a *Col6a3* exon 16 deletion mouse strain to serve as an animal model for dominant UCMD. We have demonstrated that the heterozygous mice exhibit myopathic histopathology, ultrastructural abnormalities in muscle and tendon and compromised muscle functions. Overall, the heterozygous *Col6a3* exon 16 mice display a milder phenotype than UCMD patients with an analogous molecular defect. Nevertheless, the mutant mouse recapitulates many features of UCMD and will be a valuable tool to better understand the pathogenic mechanisms of dominant UCMD and develop treatment strategies.

Acknowledgment—We thank Dr. Ken-Ichi Matsumoto for providing antibodies.

REFERENCES

1. Engel, J., Furthmayr, H., Odermatt, E., von der Mark, H., Aumailley, M., Fleischmajer, R., and Timpl, R. (1985) Structure and macromolecular organization of type VI collagen. *Ann. N.Y. Acad. Sci.* **460,** 25–37
2. Chu, M. L., Conway, D., Pan, T. C., Baldwin, C., Mann, K., Deutzmann, R., and Timpl, R. (1988) Amino acid sequence of the triple-helical domain of human collagen type VI. *J. Biol. Chem.* **263,** 18601–18606
3. Chu, M. L., Zhang, R. Z., Pan, T. C., Stokes, D., Conway, D., Kuo, H. J., Glanville, R., Mayer, U., Mann, K., and Deutzmann, R. (1990) Mosaic structure of globular domains in the human type VI collagen α3 chain. Similarity to von Willebrand factor, fibronectin, actin, salivary proteins, and aprotinin type protease inhibitors. *EMBO J.* **9,** 385–393
4. Chu, M. L., Pan, T. C., Conway, D., Kuo, H. J., Glanville, R. W., Timpl, R., Mann, K., and Deutzmann, R. (1989) Sequence analysis of α1(VI) and α2(VI) chains of human type VI collagen reveals internal triplication of globular domains similar to the A domains of von Willebrand factor and two α2(VI) chain variants that differ in the carboxy terminus. *EMBO J.* **8,** 1939–1946
5. Gara, S. K., Grumati, P., Urciuolo, A., Bonaldo, P., Kobbe, B., Koch, M., Paulsson, M., and Wagener, R. (2008) Three novel collagen VI chains with high homology to the α3 chain. *J. Biol. Chem.* **283,** 10658–10670
6. Fitzgerald, J., Rich, C., Zhou, F. H., and Hansen, U. (2008) Three novel collagen VI chains, α4(VI), α5(VI), and α6(VI). *J. Biol. Chem.* **283,** 20170–20180
7. Gara, S. K., Grumati, P., Squarzoni, S., Sabatelli, P., Urciuolo, A., Bonaldo, P., Paulsson, M., and Wagener, R. (2011) Differential and restricted expression of novel collagen VI chains in mouse. *Matrix Biol.* **30,** 248–257
8. Bönnemann, C. G. (2011) The collagen VI-related myopathies. Muscle meets its matrix. *Nat. Rev. Neurol.* **7,** 379–390
9. Allamand, V., Briñas, L., Richard, P., Stojkovic, T., Quijano-Roy, S., and Bonne, G. (2011) ColVI myopathies. Where do we stand, where do we go? *Skelet. Muscle* **1,** 30
10. Norwood, F. L., Harling, C., Chinnery, P. F., Eagle, M., Bushby, K., and Straub, V. (2009) Prevalence of genetic muscle disease in Northern England. In-depth analysis of a muscle clinic population. *Brain* **132,** 3175–3186
11. Okada, M., Kawahara, G., Noguchi, S., Sugie, K., Murayama, K., Nonaka, I., Hayashi, Y. K., and Nishino, I. (2007) Primary collagen VI deficiency is the second most common congenital muscular dystrophy in Japan. *Neurology* **69,** 1035–1042
12. Mercuri, E., and Muntoni, F. (2012) The ever-expanding spectrum of congenital muscular dystrophies. *Ann. Neurol.* **72,** 9–17
13. Briñas, L., Richard, P., Quijano-Roy, S., Gartioux, C., Ledeuil, C., Lacène, E., Makri, S., Ferreiro, A., Maugenre, S., Topaloglu, H., Haliloglu, G., Pénisson-Besnier, I., Jeannet, P. Y., Merlini, L., Navarro, C., Toutain, A., Chaigne, D., Desguerre, I., de Die-Smulders, C., Dunand, M., Echenne, B., Eymard, B., Kuntzer, T., Maincent, K., Mayer, M., Plessis, G., Rivier, F., Roelens, F., Stojkovic, T., Taratuto, A. L., Lubieniecki, F., Monges, S., Tranchant, C., Viollet, L., Romero, N. B., Estournet, B., Guicheney, P., and Allamand, V. (2010) Early onset collagen VI myopathies. Genetic and clinical correlations. *Ann. Neurol.* **68,** 511–520
14. Jöbsis, G. J., Boers, J. M., Barth, P. G., and de Visser, M. (1999) Bethlem myopathy. A slowly progressive congenital muscular dystrophy with contractures. *Brain* **122,** 649–655
15. Merlini, L., Martoni, E., Grumati, P., Sabatelli, P., Squarzoni, S., Urciuolo, A., Ferlini, A., Gualandi, F., and Bonaldo, P. (2008) Autosomal recessive myosclerosis myopathy is a collagen VI disorder. *Neurology* **71,** 1245–1253
16. Scacheri, P. C., Gillanders, E. M., Subramony, S. H., Vedanarayanan, V., Crowe, C. A., Thakore, N., Bingler, M., and Hoffman, E. P. (2002) Novel mutations in collagen VI genes. Expansion of the Bethlem myopathy phenotype. *Neurology* **58,** 593–602
17. Camacho Vanegas, O., Bertini, E., Zhang, R. Z., Petrini, S., Minosse, C., Sabatelli, P., Giusti, B., Chu, M. L., and Pepe, G. (2001) Ullrich scleroatonic muscular dystrophy is caused by recessive mutations in collagen type VI. *Proc. Natl. Acad. Sci. U.S.A.* **98,** 7516–7521
18. Pan, T. C., Zhang, R. Z., Sudano, D. G., Marie, S. K., Bönnemann, C. G., and Chu, M. L. (2003) New molecular mechanism for Ullrich congenital muscular dystrophy. A heterozygous in-frame deletion in the COL6A1 gene causes a severe phenotype. *Am. J. Hum. Genet.* **73,** 355–369
19. Zhang, R. Z., Sabatelli, P., Pan, T. C., Squarzoni, S., Mattioli, E., Bertini, E., Pepe, G., and Chu, M. L. (2002) Effects on collagen VI mRNA stability and microfibrillar assembly of three COL6A2 mutations in two families with Ullrich congenital muscular dystrophy. *J. Biol. Chem.* **277,** 43557–43564
20. Peat, R. A., Baker, N. L., Jones, K. J., North, K. N., and Lamandé, S. R. (2007) Variable penetrance of COL6A1 null mutations. Implications for prenatal diagnosis and genetic counselling in Ullrich congenital muscular dystrophy families. *Neuromuscul. Disord.* **17,** 547–557
21. Bonaldo, P., Braghetta, P., Zanetti, M., Piccolo, S., Volpin, D., and Bressan, G. M. (1998) Collagen VI deficiency induces early onset myopathy in the mouse. An animal model for Bethlem myopathy. *Hum. Mol. Genet.* **7,** 2135–2140
22. Pan, T. C., Zhang, R. Z., Markova, D., Arita, M., Zhang, Y., Bogdanovich, S., Khurana, T. S., Bönnemann, C. G., Birk, D. E., and Chu, M. L. (2013) COL6A3 protein deficiency in mice leads to muscle and tendon defects similar to human collagen VI congenital muscular dystrophy. *J. Biol. Chem.* **288,** 14320–14331
23. Lampe, A. K., Zou, Y., Sudano, D., O'Brien, K. K., Hicks, D., Laval, S. H., Charlton, R., Jimenez-Mallebrera, C., Zhang, R. Z., Finkel, R. S., Tennekoon, G., Schreiber, G., van der Knaap, M. S., Marks, H., Straub, V., Flanigan, K. M., Chu, M. L., Muntoni, F., Bushby, K. M., and Bönnemann, C. G. (2008) Exon skipping mutations in collagen VI are common and are predictive for severity and inheritance. *Hum. Mutat.* **29,** 809–822
24. Giusti, B., Lucarini, L., Pietroni, V., Lucioli, S., Bandinelli, B., Sabatelli, P., Squarzoni, S., Petrini, S., Gartioux, C., Talim, B., Roelens, F., Merlini, L., Topaloglu, H., Bertini, E., Guicheney, P., and Pepe, G. (2005) Dominant and recessive COL6A1 mutations in Ullrich scleroatonic muscular dystrophy. *Ann. Neurol.* **58,** 400–410
25. Baker, N. L., Mörgelin, M., Peat, R., Goemans, N., North, K. N., Bateman, J. F., and Lamandé, S. R. (2005) Dominant collagen VI mutations are a common cause of Ullrich congenital muscular dystrophy. *Hum. Mol. Genet.* **14,** 279–293
26. Tillet, E., Wiedemann, H., Golbik, R., Pan, T. C., Zhang, R. Z., Mann, K., Chu, M. L., and Timpl, R. (1994) Recombinant expression and structural and binding properties of α1(VI) and α2(VI) chains of human collagen type VI. *Eur. J. Biochem.* **221,** 177–185
27. Specks, U., Mayer, U., Nischt, R., Spissinger, T., Mann, K., Timpl, R., Engel, J., and Chu, M. L. (1992) Structure of recombinant N-terminal globule of type VI collagen α3 chain and its binding to heparin and hyaluronan. *EMBO J.* **11,** 4281–4290
28. Bogdanovich, S., Krag, T. O., Barton, E. R., Morris, L. D., Whittemore, L. A., Ahima, R. S., and Khurana, T. S. (2002) Functional improvement of dystrophic muscle by myostatin blockade. *Nature* **420,** 418–421
29. Bogdanovich, S., McNally, E. M., and Khurana, T. S. (2008) Myostatin

blockade improves function but not histopathology in a murine model of limb-girdle muscular dystrophy 2C. *Muscle Nerve* **37,** 308–316
30. Brooks, S. V., and Faulkner, J. A. (1990) Contraction-induced injury. Recovery of skeletal muscles in young and old mice. *Am. J. Physiol.* **258,** C436–C442
31. Izu, Y., Ansorge, H. L., Zhang, G., Soslowsky, L. J., Bonaldo, P., Chu, M. L., and Birk, D. E. (2011) Dysfunctional tendon collagen fibrillogenesis in collagen VI null mice. *Matrix Biol.* **30,** 53–61
32. Norris, R. A., Damon, B., Mironov, V., Kasyanov, V., Ramamurthi, A., Moreno-Rodriguez, R., Trusk, T., Potts, J. D., Goodwin, R. L., Davis, J., Hoffman, S., Wen, X., Sugi, Y., Kern, C. B., Mjaatvedt, C. H., Turner, D. K., Oka, T., Conway, S. J., Molkentin, J. D., Forgacs, G., and Markwald, R. R. (2007) Periostin regulates collagen fibrillogenesis and the biomechanical properties of connective tissues. *J. Cell Biochem.* **101,** 695–711
33. Irwin, W. A., Bergamin, N., Sabatelli, P., Reggiani, C., Megighian, A., Merlini, L., Braghetta, P., Columbaro, M., Volpin, D., Bressan, G. M., Bernardi, P., and Bonaldo, P. (2003) Mitochondrial dysfunction and apoptosis in myopathic mice with collagen VI deficiency. *Nat. Genet.* **35,** 367–371
34. Lamandé, S. R., Mörgelin, M., Selan, C., Jöbsis, G. J., Baas, F., and Bateman, J. F. (2002) Kinked collagen VI tetramers and reduced microfibril formation as a result of Bethlem myopathy and introduced triple helical glycine mutations. *J. Biol. Chem.* **277,** 1949–1956
35. Persikov, A. V., Ramshaw, J. A., Kirkpatrick, A., and Brodsky, B. (2000) Amino acid propensities for the collagen triple-helix. *Biochemistry* **39,** 14960–14967
36. Sabatelli, P., Gualandi, F., Gara, S. K., Grumati, P., Zamparelli, A., Martoni, E., Pellegrini, C., Merlini, L., Ferlini, A., Bonaldo, P., Maraldi, N. M., Paulsson, M., Squarzoni, S., and Wagener, R. (2012) Expression of collagen VI α5 and α6 chains in human muscle and in Duchenne muscular dystrophy-related muscle fibrosis. *Matrix Biol.* **31,** 187–196
37. Sacco, A., Mourkioti, F., Tran, R., Choi, J., Llewellyn, M., Kraft, P., Shkreli, M., Delp, S., Pomerantz, J. H., Artandi, S. E., and Blau, H. M. (2010) Short telomeres and stem cell exhaustion model Duchenne muscular dystrophy in mdx/mTR mice. *Cell* **143,** 1059–1071
38. Angelin, A., Tiepolo, T., Sabatelli, P., Grumati, P., Bergamin, N., Golfieri, C., Mattioli, E., Gualandi, F., Ferlini, A., Merlini, L., Maraldi, N. M., Bonaldo, P., and Bernardi, P. (2007) Mitochondrial dysfunction in the pathogenesis of Ullrich congenital muscular dystrophy and prospective therapy with cyclosporins. *Proc. Natl. Acad. Sci. U.S.A.* **104,** 991–996
39. Merlini, L., Angelin, A., Tiepolo, T., Braghetta, P., Sabatelli, P., Zamparelli, A., Ferlini, A., Maraldi, N. M., Bonaldo, P., and Bernardi, P. (2008) Cyclosporin A corrects mitochondrial dysfunction and muscle apoptosis in patients with collagen VI myopathies. *Proc. Natl. Acad. Sci. U.S.A.* **105,** 5225–5229
40. Gualandi, F., Manzati, E., Sabatelli, P., Passarelli, C., Bovolenta, M., Pellegrini, C., Perrone, D., Squarzoni, S., Pegoraro, E., Bonaldo, P., and Ferlini, A. (2012) Antisense-induced messenger depletion corrects a COL6A2 dominant mutation in Ullrich myopathy. *Hum. Gene Ther.* **23,** 1313–1318
41. Minamitani, T., Ikuta, T., Saito, Y., Takebe, G., Sato, M., Sawa, H., Nishimura, T., Nakamura, F., Takahashi, K., Ariga, H., and Matsumoto, K. (2004) Modulation of collagen fibrillogenesis by tenascin-X and type VI collagen. *Exp. Cell Res.* **298,** 305–315
42. Urciuolo, A., Quarta, M., Morbidoni, V., Gattazzo, F., Molon, S., Grumati, P., Montemurro, F., Tedesco, F. S., Blaauw, B., Cossu, G., Vozzi, G., Rando, T. A., and Bonaldo, P. (2013) Collagen VI regulates satellite cell self-renewal and muscle regeneration. *Nat. Commun.* **4,** 1964
43. Schalkwijk, J., Zweers, M. C., Steijlen, P. M., Dean, W. B., Taylor, G., van Vlijmen, I. M., van Haren, B., Miller, W. L., and Bristow, J. (2001) A recessive form of the Ehlers-Danlos syndrome caused by tenascin-X deficiency. *N. Engl. J. Med.* **345,** 1167–1175
44. Kirschner, J., Hausser, I., Zou, Y., Schreiber, G., Christen, H. J., Brown, S. C., Anton-Lamprecht, I., Muntoni, F., Hanefeld, F., and Bönnemann, C. G. (2005) Ullrich congenital muscular dystrophy. Connective tissue abnormalities in the skin support overlap with Ehlers-Danlos syndromes. *Am. J. Med. Genet. A* **132A,** 296–301
45. Minamitani, T., Ariga, H., and Matsumoto, K. (2004) Deficiency of tenascin-X causes a decrease in the level of expression of type VI collagen. *Exp. Cell Res.* **297,** 49–60
46. Voermans, N. C., Verrijp, K., Eshuis, L., Balemans, M. C., Egging, D., Sterrenburg, E., van Rooij, I. A., van der Laak, J. A., Schalkwijk, J., van der Maarel, S. M., Lammens, M., and van Engelen, B. G. (2011) Mild muscular features in tenascin-X knockout mice, a model of Ehlers-danlos syndrome. *Connect. Tissue Res.* **52,** 422–432
47. Lorts, A., Schwanekamp, J. A., Baudino, T. A., McNally, E. M., and Molkentin, J. D. (2012) Deletion of periostin reduces muscular dystrophy and fibrosis in mice by modulating the transforming growth factor-β pathway. *Proc. Natl. Acad. Sci. U.S.A.* **109,** 10978–10983
48. Ritty, T. M., Roth, R., and Heuser, J. E. (2003) Tendon cell array isolation reveals a previously unknown fibrillin-2-containing macromolecular assembly. *Structure* **11,** 1179–1188
49. Wiberg, C., Hedbom, E., Khairullina, A., Lamandé, S. R., Oldberg, A., Timpl, R., Mörgelin, M., and Heinegård, D. (2001) Biglycan and decorin bind close to the N-terminal region of the collagen VI triple helix. *J. Biol. Chem.* **276,** 18947–18952
50. Chen, S., and Birk, D. E. (2013) The regulatory roles of small leucine-rich proteoglycans in extracellular matrix assembly. *FEBS J.* **280,** 2120–2137